

Early secreted antigenic target of 6-kDa of *Mycobacterium tuberculosis* induces transition of macrophages into epithelioid macrophages by downregulating iNOS / NO-mediated H3K27 trimethylation in macrophages

Jiahui Lin^{a,b}, Yuyin Jiang^{a,b}, Dan Liu^{a,b}, Xueting Dai^b, Min Wang^{a,b}, Yalei Dai^{a,b,*}

^a Shanghai Key Lab of Tuberculosis, Shanghai Pulmonary Hospital, School of Medicine, Tongji University, 507 Zhengmin Road, Shanghai, 200433, China

^b Department of Microbiology and Immunology, School of Medicine, Tongji University, 1239 Siping Road, Shanghai, 200092, China

ARTICLE INFO

Keywords:

Macrophage
Granuloma
ESAT6
TLR2
NO
H3K27me3

ABSTRACT

Background: Tuberculosis (TB) is a chronic infectious disease caused by *Mycobacterium tuberculosis* (Mtb). Granuloma is a pathological feature of tuberculosis and is a tight immune cell aggregation caused by Mtb. The main constituent cells are macrophages and their derivative cells including epithelioid macrophages. However, the molecular mechanism of the transition has not been reported. The purpose of this study was to investigate whether early secreted antigenic target of 6-kDa (ESAT6) can induce the transition of bone marrow-derived macrophages (BMDMs) into epithelioid macrophages and its possible molecular mechanism.

Methods: The recombinant ESAT6 protein was obtained from *E. coli* carrying *esat6* gene after isopropyl β-D-thiogalactopyranoside (IPTG) induction. BMDMs were isolated from bone marrow of mice hind legs. Cells viability was detected by Cell Counting Kit 8 (CCK8) assays. The expression levels of mRNA and proteins were detected by qPCR and Western blot, or evaluated by flow cytometry. The expression level of nitric oxide (NO) was measured with a nitric oxide indicator.

Results: ESAT6 could significantly induce mRNA and protein expression levels of a group of epithelioid macrophages marker molecules (EMMMs), including E-cadherin, junction plakoglobin, ZO1, desmoplakin, desmoglein3 and catenin proteins, in BMDMs. These events could be abrogated in macrophage from TLR2 deficiency mice. ESAT6 could also markedly induce iNOS/NO production that could significantly inhibit trimethylation of H3K27 in the cells. ESAT6-induced expressions of epithelioid macrophages marker molecules were significantly inhibited in the presence of H3K27 histone demethylase inhibitor GSK J1. Furthermore, ROS scavenging agent N,N'-Dimethylthiourea (DMTU) could markedly inhibit the transition induced by ESAT6 in macrophages.

Conclusion: This study demonstrates that ESAT6 bound with TLR2 can activate iNOS/NO and ROS signalings to reduce the trimethylation of H3K27 resulting in the increment of EMMM expression that is beneficial to the transition of macrophages into epithelioid macrophages. However, hypoxia can inhibit this transition event. This study has provided new evidence of pathogenesis of granuloma caused by Mtb and also proposed new ideas for the treatment of TB.

1. Introduction

Tuberculosis (TB) is a chronic infectious disease caused by mycobacterium tuberculosis (Mtb), usually the bacillus invades human lungs

(about 85 % of cases) (Van Zyl et al., 2015). In addition, tuberculosis is a complex disease and more than 90 % of people infected could spontaneously control. There is a certain correlation between the development of tuberculosis and the individual immunity status, and people

Abbreviations: BMDM, bone marrow-derived macrophage; EMMM, epithelioid macrophages marker molecule; TLR2, Toll like receptor 2; MMP9, matrix metalloproteinase-9; Mtb, *Mycobacterium tuberculosis*; ESAT6, early secreted antigenic target of 6-kDa; CFP10, culture filtrate protein-10; BCG, Bacille Calmette-Guérin; NO, nitric oxide; iNOS, inducible nitric oxide synthase; ROS, reactive oxygen species; RNI, reactive nitrogen intermediate; H3K27me3, trimethylated lysine 27 on histone H3; SDS-PAGE, sodium dodecyl sulfate polyacrylamide gel electrophoresis; ECL, enhanced chemiluminescence; CCK8, cell counting kit 8; FACS, fluorescence-activated cell sorter; GAPDH, glyceraldehyde-3-phosphate dehydrogenase; BCA, bicinchoninic acid; IPTG, isopropyl β-D-thiogalactopyranoside; SMT, (S)-methylsiothiourea sulfate; PTIO, crboxy-PTIO potassium salt; DMTU, N,N'-dimethylthiourea

* Corresponding author at: Shanghai Key Lab of Tuberculosis, Shanghai Pulmonary Hospital, Department of Microbiology and Immunology, School of Medicine, Tongji University, China.

E-mail address: daiyl@tongji.edu.cn (Y. Dai).

<https://doi.org/10.1016/j.molimm.2019.11.013>

Received 14 June 2019; Received in revised form 31 October 2019; Accepted 30 November 2019

0161-5890/ © 2019 Elsevier Ltd. All rights reserved.

with low immunity are more susceptible to Mtb (Cambier et al., 2014). Macrophages, as an important effector in immune response, are the main cell type found in the tuberculous granuloma and have high plasticity. It has been reported that macrophages can transdifferentiate into various cells such as epithelioid macrophages, foam cells and multinuclear giant cells (Silva Miranda et al., 2012; Russell et al., 2009). With adaptive immunity to disease onset, granulomas become more solid, in which infected macrophages are surrounded by layers of immune cells including dendritic cells, natural killer cells, and T and B lymphocytes (Eum et al., 2010).

The formation of granuloma is mainly caused by complex mechanisms including the epithelial reprogramming in granuloma formation and the migration of macrophages within the lesion. The mechanism of this event during Mtb infection has not been fully reported. It has been reported ESAT6 of Mtb can stimulate epithelial cells to express MMP9 that can degrade all components of extracellular matrix, which may enable macrophage migration to infected site forming granuloma (Volkman et al., 2010). A study of zebrafish infection model proved that the epithelioid macrophages that make up the granuloma are derived from infected macrophages (Cronan et al., 2016). From images of zebrafish's embryos acquired through its optical transparency, it can be seen clearly that only macrophages are aggregated around *M. marinum* infection region since the embryo does not have lymphocytes (Volkman et al., 2004). More than 12 specific molecules of epithelioid macrophages have been identified in the zebrafish infection model. However, the molecular mechanism of the transition has not been reported.

Mycobacillus-macrophage interactions can trigger granulomatous formation only in the context of innate immunity. Bacille Calmette-Guérin (BCG) is an attenuated strain of mycobacterium bovis that is used as a vaccine against tuberculosis for many years. Genetic studies have identified the differences in Mtb DNA region between H37Rv strain and BCG. It has been reported that both RD1 (region of difference 1) and RD9 (region of difference 9) have been deleted in BCG compared with that in H37Rv strain (Teo et al., 2013). More studies showed both H37Rv- Δ RD1 and BCG present low-virulence, revealing the RD1 gene encoding protein helps to enhance virulence Mtb infection in mice infection model (Brosch et al., 2002; Sherman et al., 2004). In immunodeficient mice, both BCG :: RD1 and *M. microti* :: RD1 knock-in increased the number of bacteria compared with the control group, and induced extensive splenomegaly and granuloma formation, indicating that RD1 is conducive to the formation of granuloma (Pym et al., 2002). Recent studies in zebrafish model, compared with wild-type bacteria, *M. marinum*- Δ RD1 infection showed fewer granuloma formation, mainly produced a necrosis, loose macrophage aggregates (Volkman et al., 2004). Taken together, those studies indicate that RD1 contributes to the formation of granuloma and the virulence of Mtb.

RD1 is considered to be of a vital important region that encodes nine proteins in Mtb (Rv3871 to Rv3879c), and contains the secretory system named type VII secretory system. Some or all the products encoded by RD1 gene may be involved in virulence and pathogenesis. Among them, the hot research area is Rv3874 encoding culture filtrate protein-10 (CFP10), and Rv3875 encoding ESAT6. Both of them can induce strong innate and adaptive immunity in laboratory animals and human. The two proteins are transported out of the bacteria in a 1:1 dimer structure and disintegrated in the external environment. The role of CFP10 has not been fully reported, and ESAT6, as the virulence protein of Mtb, regulates the immune balance through the interaction with immune cells to promote the infection of Mtb. It has been reported that ESAT6 is involved in the establishment of early infection of endobacterium macrophage and plays an important role in the virulence of Mtb (Brodin et al., 2004).

Nitric oxide (NO) and Reactive nitrogen intermediate (RNI) not only are effective bacteriostatic molecules but also act as signal transducers. The Mtb infection model of NOS2 deficient mice showed that RNI could regulate Mtb gene expression in vivo (Ohno et al., 2003). It has been

reported that iNOS/NO is an important signaling molecule of epithelioid cells (Gharun et al., 2018). In tuberculous granuloma, epithelioid cells co-locate with inducible nitric oxide synthase (iNOS), and the formation of NO induces the differentiation of macrophages in a non-viral methodology to transdifferentiate fibroblasts to induced epithelial cells (Meng et al., 2016). More importantly, trimethylated lysine 27 on histone H3 (H3K27me3) is a key factor that maintains the plasticity of macrophages. A study reported that the expression of H3K27me3 is closely related to the status of epithelial cells (Yang et al., 2009). More and more evidence shows that the epithelial-mesenchymal transdifferentiation of tumor cells depends on the upregulation of H3K27me3 (Ke et al., 2010). These findings suggest that the downregulation of H3K27me3 could control the expression of epithelial cells-related proteins.

To understand how ESAT6 is related to the macrophage transition, this study investigated the role of ESAT6 in inducing the expression of EMMs that may be involved in macrophage epithelial reprogramming. ESAT6-mediated transition signal pathways are explored. Meanwhile, the hypoxia effects on the transition are also studied.

2. Materials and methods

2.1. Reagents

Commercial standard ESAT6 was purchased from ProSpec-Tany Technogene Ltd (Ness Ziona, Israel). E-Toxate kit for LPS detection and the endotoxin removal kit were purchased from Bioendo (Xiamen, China). FITC-tagged mAbs against mouse F4/80 and Alexa Fluor® 488 were obtained from Jackson (West Grove, PA, USA). Sodium dodecyl sulfate-polyacrylamide gel (SDS-PAGE gel) kit was purchased from EpiZyme (Shanghai, China). SYBR Premix Ex Taq™II and PrimeScript™ RT Master Mix were purchased from Takara (Shiga, Japan). Rabbit anti-mouse E-Cadherin, ZO1, H3K27me3, iNOS and GADPH antibodies were obtained from Abcam (Cambridge, UK). The Griess Reaction kit was purchased from Beyotime (Shanghai, China). H3K27 histone demethylase inhibitor GSK J1 and iNOS inhibitor (S)-Methylisothiourea sulfate (SMT) were purchased from Selleck (Houston, TX, USA). NO inhibitor Carboxy-PTIO potassium salt PTIO and general laboratory chemicals were obtained from Sangon (Shanghai, China).

2.2. Preparation of recombinant ESAT6

Recombinant ESAT6 was expressed and purified from the pET21a/BL21 system as described previously (Liu et al., 2014). Briefly, BL21 cells, containing the plasmid pET21a/*esat6* with polyhistidine-tagged recombinant ESAT6 expressed as a soluble protein in *E. coli*, were grown in Luria-Bertani medium and induced with a final concentration of 1 mM IPTG for 3 h. After ultrasonication, the production of the recombinant ESAT6 was purified through a Nickel-nitrilotriacetic (Ni-NTA) purification system according to the manufacturer's recommendations (Sangon, Shanghai, China). The purity of the recombinant ESAT6 in the eluted fractions was determined by SDS-PAGE (12.5 % gel). The contaminated endotoxin in the recombinant ESAT6 was removed by endotoxin removal kit and LPS in the protein was less than 20 pg/mg that has no effect on E-cadherin and ZO1 expression. The biological activity of the recombinant ESAT6 was compared with commercial standard ESAT6. The stock solution of the recombinant ESAT6 was aliquoted and stored at -80°C for further studies.

2.3. Isolation and culture of bone marrow derived macrophage (BMDM)

C57BL/6 mice (6–8 weeks, male) were purchased from the Animal Center of Tongji University (Shanghai, China). The mice were sacrificed by cervical dislocation. BMDMs were isolated by flushing the bone marrow of hind legs with RPMI 1640 medium after sterilizing the hind

legs with 75 % ethanol and PBS. The cells were washed with PBS after contaminated red blood cells were lysed. Then cells were resuspended with concentration 2×10^6 cells/ml in complete culture medium containing RPMI 1640 with 10 % FBS, 20 % L929 conditional medium, 100 U/ml penicillin, 0.1 mg/ml streptomycin. The cells were cultured in a humidified incubator with 5 % CO₂ at 37 °C and allowed to fully differentiate for 6 days before being used for experiments. This project involving mice has been approved by the Institutional Ethics Committee of Animal Experimentation of Tongji University. All protocols complied with the National Institutes of Health Guide for the care and use of laboratory animals, and conformed to directive 2010/63/EU and NIH guidelines.

2.4. Cell counting kit 8 assays

Detection of ESAT6 protein cytotoxicity followed the manufacturer's instructions of Cell Counting Kit 8 (CCK8). Briefly, cells were cultured in 96-well culture plates with 100 µl culture medium and stimulated with ESAT6 in a concentration range indicated for 24 h, then 10 µl of CCK 8 test solution was added and further incubated for 4 h. The absorbance of each well was measured at 450 nm using a microplate reader. The OD data were obtained and analyzed. The IC50 value of the cell was calculated.

2.5. Immunofluorescence staining

Slider-cultured cells were fixed with 4 % paraformaldehyde for 15 min followed by permeabilization with 0.2 % Triton X-100 in 1 × PBS for 5 min at room temperature. Then cells were washed in ice-cold PBS and blocked with 5 % donkey serum in PBS for 60 min before the slides were immune-stained with the primary antibody and the fluorescent-labeled secondary antibody. Composites of images were assembled and labeled using Photoshop software.

2.6. Cell transwell assays

Cell migration assays were performed using multi-well chambers with 8 µm pores (Millipore, Massachusetts, MA, USA). According to experiment design, the cells were pre-incubated with or without 3 µl/ml ESAT6 for 24 h before passaging into the upper chamber with a concentration 1.5×10^5 cells/well. The upper wells contain 5 % FBS in basal medium while bottom wells with 10 % FBS in basal medium. The cells were incubated for 3 h before scrapping off none-migrate cells on the surface of the upper chamber membrane. The migrated cells were stained with crystal violet and subsequently counted under three randomly chosen high power fields (400×).

2.7. Flow cytometry

Cells were grown to 80 % confluence in 60 mm² dishes and treated with ESAT6 according to experiment design. Then cells were incubated with blocking solution containing 2 % mouse serum for 15 min and washed with PBS once before being resuspended with FACS buffer (5 % FBS in PBS). The cells were then incubated with fluorescent-labeled primary antibodies. The flow cytometry analysis was performed using FACScan. A minimum of 10000-gated cells was collected per sample. The fluorescent intensity per sample was analyzed using Flow Jo software.

2.8. SDS-PAGE and Western blot

Cells were cultured in 60 mm² dishes and grown to 80 % confluence before experiments. At the end of each experiment, the total proteins were harvested in RIPA lysis buffer on ice. Protein levels were determined using BCA protein assay kit. Equal amount of extracted protein (40 mg/lane) were separated in SDS-PAGE gels. For Coomassie

Table 1

A list of sense and antisense primers for qPCR.

Abbreviation	Genes	Primer sequence
cdh1	E-Cadherin	F 5'-TGCCATAGTGGGATATGTTG-3' R 5'-TGAAGAAGACGCCAAGAAG-3'
jup	Junction Plakoglobin	F 5'-TTGTTCCGGTACTGAGTTGC-3' R 5'-GGCTGCTCAATAAGGTTTCAT-3'
tjp	ZO1 (tight junction protein)	F 5'-TATTATGGCACATCAGCAGC-3' R 5'-AGAAATCCTTTCACACCTACTG-3'
dsp	Desmoplakin	F 5'-TCCTAGAGCCTGAAGCAA-3' R 5'-CGAAGCCTGAGCAGAGT-3'
dsg3	Desmoglein-3	F 5'-GTACAAACGTGAATGGGTGA-3' R 5'-AATCCCACTCCAGAAATGC-3'
ctnnd1	Catenin	F 5'-GTCTTCTCAGCACATTGGT-3' R 5'-TGTTAAGAGAAGGCCCGTAA-3'
gadh	GADPH	F: 5'-CAATACGCCAAATCCGTTG-3' R: 5'-CGCATCTTCTTTGCGTC-3'

blue staining, the gel was stained with Coomassie Blue Fast Staining Solution. For Western blot, the proteins were transferred to polyvinylidene difluoride membrane. The membranes were blocked with 5 % bovine serum albumin (BSA) before being probed with primary and secondary antibodies in 5 % BSA in TBST. The protein levels were detected using Clarity Western ECL Substrate (Millipore, Billerica, MA, USA). Quantification of each band was performed by measuring the gray value using ImageJ software (National Institutes of Health, Bethesda, MD, USA).

2.9. qPCR analysis

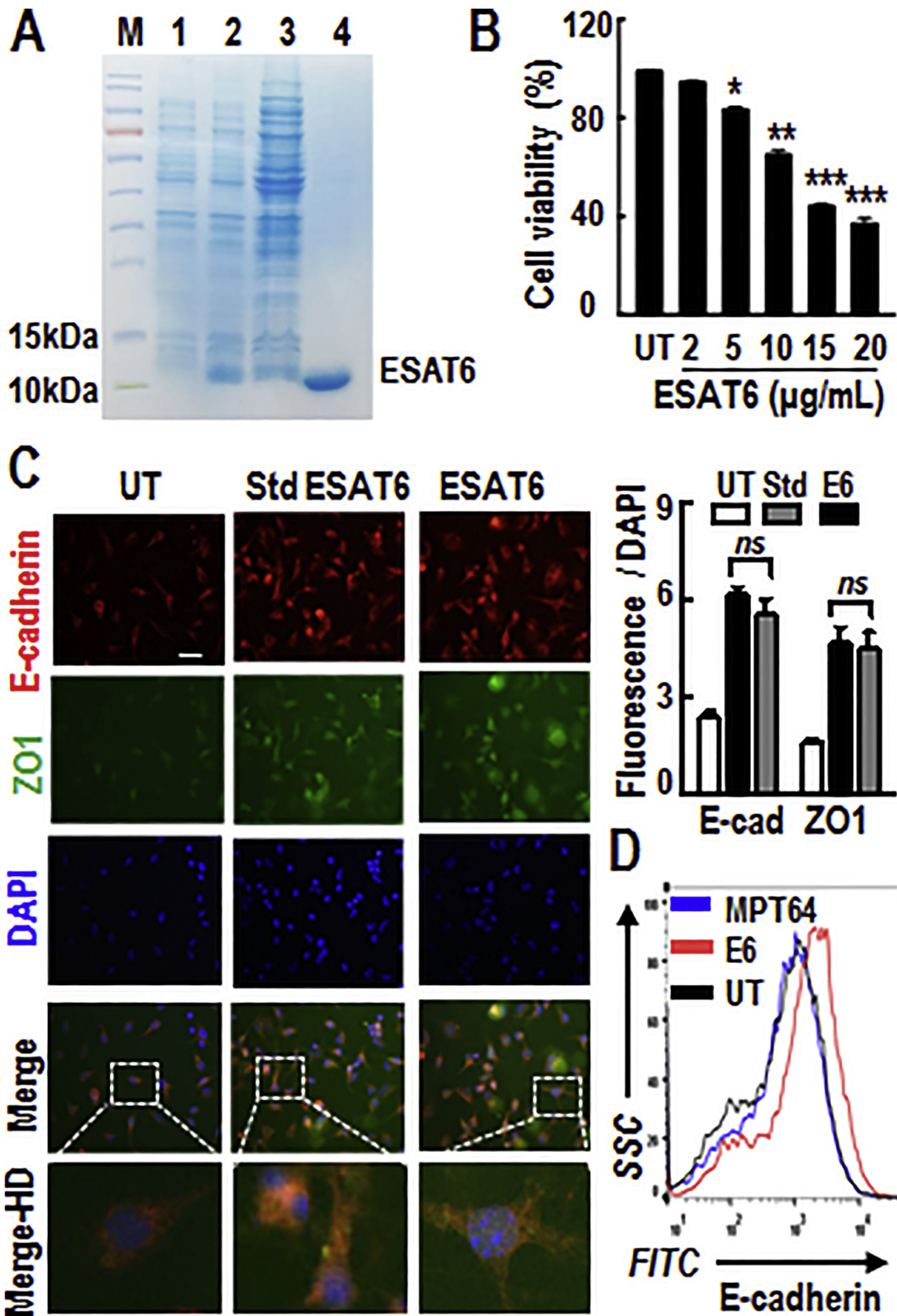
Total RNA was extracted from BMDMs as previously described (Liu et al., 2014). The RNA was reversed to cDNA by using PrimeScript RT Master Mix. RT products (cDNA) were amplified by Applied Biosystems 7500 Real-Time PCR systems with Power SYBR green Master Mix. The mRNA transcription levels were detected by PCR amplification of cDNA using the following sense and antisense primers in Table 1. At the end of the amplification, cycle threshold values were normalized to those obtained for GAPDH, and $2^{-\Delta\Delta Ct}$ was used to calculate change in relative mRNA expression between groups, which were calculated from the equations as follow: $2^{-\Delta\Delta Ct} = 2^{-\Delta Ct (Sample) - \Delta Ct (Control)}$, while $\Delta Ct (Sample) = Ct (Sample, Genes) - Ct (Sample, GAPDH)$, $\Delta Ct (Control) = Ct (Control, Genes) - Ct (Control, GAPDH)$.

2.10. Nitric oxide detection

Cells were cultured in 6-well plates and stimulated with 3 µg/ml ESAT6 for the indicated time periods. Nitric oxide (NO) was measured in cell supernatants using Griess Reaction kit. Briefly, in the 96-well plate, 50 µl standard substance and supernatant were added to each well, then 50 µl Griess Reagent I was added followed by 50 µl Griess Reagent II into each well. The absorbance was immediately determined at 540 nm using a microplate reader. The OD data were obtained and analyzed.

2.11. Reactive oxygen species detection

Reactive oxygen species (ROS) production were directly measured using ROS Assay Kit (KeyGen BioTECH, Nanjing, China). The cells were incubated with 3 µg/ml ESAT6 for indicated time period. After incubation, the cells were harvested and suspended in PBS containing 10 µM DCFH-DA, and stained at 37 °C for 30 min. Washed with cold PBS, the cells were the analyzed by flow cytometry. Data were analyzed with Flow Jo software.



(caption on next page)

Fig. 1. Purified Recombinant ESAT6 has the biological activity.

A. Recombinant ESAT-6 protein was purified from *E. coli* containing *east6* gene after IPTG induction. Samples were separated by 12.5 % SDS-PAGE, and the bands of proteins were visualized after Coomassie blue staining. Line 1: *E. coli* transformed with the plasmid pET21a-esat6; Line 2: transformed *E. coli* were induced by IPTG for 3 h; Line 3: supernatant collection after ultrasonic treatment of induced *E. coli*. Line 4: N-His tagged ESAT6 was purified by a Ni²⁺-affinity column. **B.** The biological activity of purified ESAT6 was tested for cell viability. BMDMs were treated with the indicated concentrations of ESAT6 for 24 h. The cell viability was detected by CCK8 assay (n = 4). *P < 0.05, **P < 0.01, ***P < 0.001 vs. untreated group. **C.** The biological activity of purified ESAT6 was compared with commercial standard ESAT6. BMDMs were stimulated with 3 µg/ml ESAT6 (E6) or Std-ESAT6 (Std) for 24 h, followed by triple staining of the cells with E-cadherin (red), ZO1 (green) and DAPI (blue). A representative group images of stained cells was observed under inverted fluorescence microscope. Bar = 50 µm. Similar results were observed in three separate experiments. The data of quantitative immunofluorescence ratio were showed (n = 3). **D.** The comparison of the efficacy between the purified ESAT6 or MPT64 proteins in inducing E-cadherin expression in BMDMs. BMDMs were incubated with 3 µg/ml purified ESAT6 or MPT64 for 24 h, then the expression levels of E-cadherin were detected by Flow cytometry. A typical E-cadherin expression on the surface of the cells were analyzed. Similar results were observed in three separate experiments from three individual mice.

2.12. Data and statistical analysis

Cell samples were from more than three individual mice and each samples were in triplicate in all experiments. Data were analyzed by using GraphPad Prism 6.0. All data were reported as mean value ± SEM. In order to assess the statistical significance of inter group differences, the unpaired two-tailed *t*-test were applied for statistical analysis. Differences with *p* value < 0.05 were considered to be statistically significant while *ns* indicates there is no significant difference.

3. Result

3.1. ESAT6 could induce the expression of E-cadherin and ZO1 molecules in BMDMs

To obtain the recombinant ESAT6 protein, *E. coli* carrying pET21a/*east6* gene plasmid was induced with IPTG and the target protein ESAT6 was expressed successfully. After purification ESAT6 protein was analyzed in SDS-PAGE gel stained with Coomassie Blue Staining, the protein was observed to have a relative molecular weight about 12 kDa (with 6xhistidine tag) (Fig.1A). The biological activity of the recombinant ESAT6 was tested for cells viability after LPS has been removed. BMDMs were incubated with the ESAT6 in a different concentration range indicated for 24 h. The results showed that BMDM viability was markedly dropped when the concentration of the ESAT6 was greater than 5 µg/ml (Fig.1B), and LD₅₀ for BMDM was about 14 µg/ml. In order to keep BMDMs growing normally, 3 µg/ml of the recombinant ESAT6 was chosen for further studies. Expressions of E-cadherin and ZO1 molecules in BMDMs were observed after BMDMs were treated with the recombinant ESAT6 or commercial standard ESAT6 (Std ESAT6) respectively. As shown in Fig.1C, the expression levels of E-cadherin and ZO1 were significantly increased in the recombinant ESAT6 treated group as well as in commercial standard ESAT6 treated group. It is expected that the increasing rates were almost unanimous for the different source of ESAT6, which indicates that the recombinant ESAT6 has the same quality as Std-ESAT6 to induce E-cadherin and ZO1 expression. There maybe trace of LPS in the recombinant ESAT6 but no biological effect was observed in this study (data not shown). Furthermore, the mock experiment showed MPT64, a 23 kDa protein derived from *Mtb*, did not stimulate E-cadherin expression on the surface of BMDM although the recombinant MPT64 was expressed and purified in the same method as the recombinant ESAT6 (Fig.1D), which indicates that the increment of E-cadherin expression is specific to the recombinant ESAT6.

The classical granulomatous of TB tend to aggregate macrophages that then evolve into epithelioid macrophages (Ramakrishnan, 2012). The molecular transition mechanism of macrophages into epithelioid macrophages in granuloma has not been reported. EMMMs expressed on macrophage may affect cell migration. In order to examine whether ESAT6 affects macrophage migration, BMDMs were treated with ESAT6 and the cells migration rate was detected. The results showed that the migration rate of ESAT6-treated cells was significantly reduced

compared with that of the untreated cells (Fig.2A). It has been reported that the expression of E-cadherin is not only regulated by a variety of factors but also affects many cell functions, and is often used as a marker protein for epithelialization (Gheldof and Berx, 2013). To identify whether E-cadherin and ZO1 molecules was involved in this event, ESAT6-induced both molecules expression were analyzed. The results showed that the E-cadherin and ZO1 expression on the surface of ESAT6-treated BMDMs were markedly increased (Fig.2B). The western blot analysis further showed that ESAT6 could induce a dose- and time-dependent pattern to upregulate E-cadherin expression in ESAT6-treated BMDMs (Fig.2C). Furthermore, by using the fluorescent-labeled antibody for tracing ZO1 expression in ESAT6-treated BMDMs, the results also showed the same time-dependent expression manner after quantitative fluorescence analyzing (Fig.2D). A previous study has identified more than 12 molecules as markers of macrophage epithelialization (Marakalala et al., 2016). To expose these related molecules, the transcriptional levels of a group of EMMM genes in ESAT6-treated BMDMs were detected by qPCR. As shown in Fig.2E, the expressed relative mRNA levels of the EMMM genes, including *cdh1*, *jup*, *tjp*, *dsp*, *dsg3*, *ctnnd1*, were significantly up-regulated in the BMDMs treated with ESAT6. These data indicate that ESAT6 has the ability to induce the transition of macrophages into epithelioid macrophages.

3.2. ESAT6-induced transition of macrophage depends on TLR2 molecule

A previous study has shown that ESAT6 bound to TLR2 can induce production of monocyte chemoattractant protein-1 and TNFα in macrophages and TLR2 is an initial molecule to pass ESAT6 signal into the cells for these events (Liu et al., 2014; Pathak et al., 2007). However, it has also been reported that ESAT6-induced IL-6 production in macrophage is not via TLR2 signal (Jung et al., 2017). To identify whether ESAT6-induced epithelioid macrophage changes are dependent on TLR2, it is necessary to examine TLR2's effect on the expression of EMMMs in the ESAT6-treated macrophages. BMDMs from WT and TLR2^{-/-} mice were stimulated with or without ESAT6, and the expression of E-cadherin on the surface of BMDMs was observed after using fluorescent-labeled antibody staining. As shown in Fig. 3A-B, the E-cadherin positive cells were markedly increased in the cells from WT mice but not in the cells from TLR2^{-/-} mice. This phenomenon was further confirmed by detecting mRNA expression levels of the group of EMMMs genes using qPCR (Fig.3C). Nevertheless, Pam3CSK4, a common TLR2 activator, can only induce low level of E-cadherin expression (data not shown). These results suggest that the induction of the high levels of EMMMs expression in ESAT6-treated macrophage requires the attendance of TLR2 on the surface of the cells.

3.3. ESAT6 induces the transition of macrophage via activation of iNOS/NO-H3K27me3

In order to understand the signal mechanism of ESAT6-induced transition of macrophage, further study is needed. It has been reported that NO acts as a signal molecule to regulate the plasticity of macrophages (Gharun et al., 2018). To examine the potential involvement of

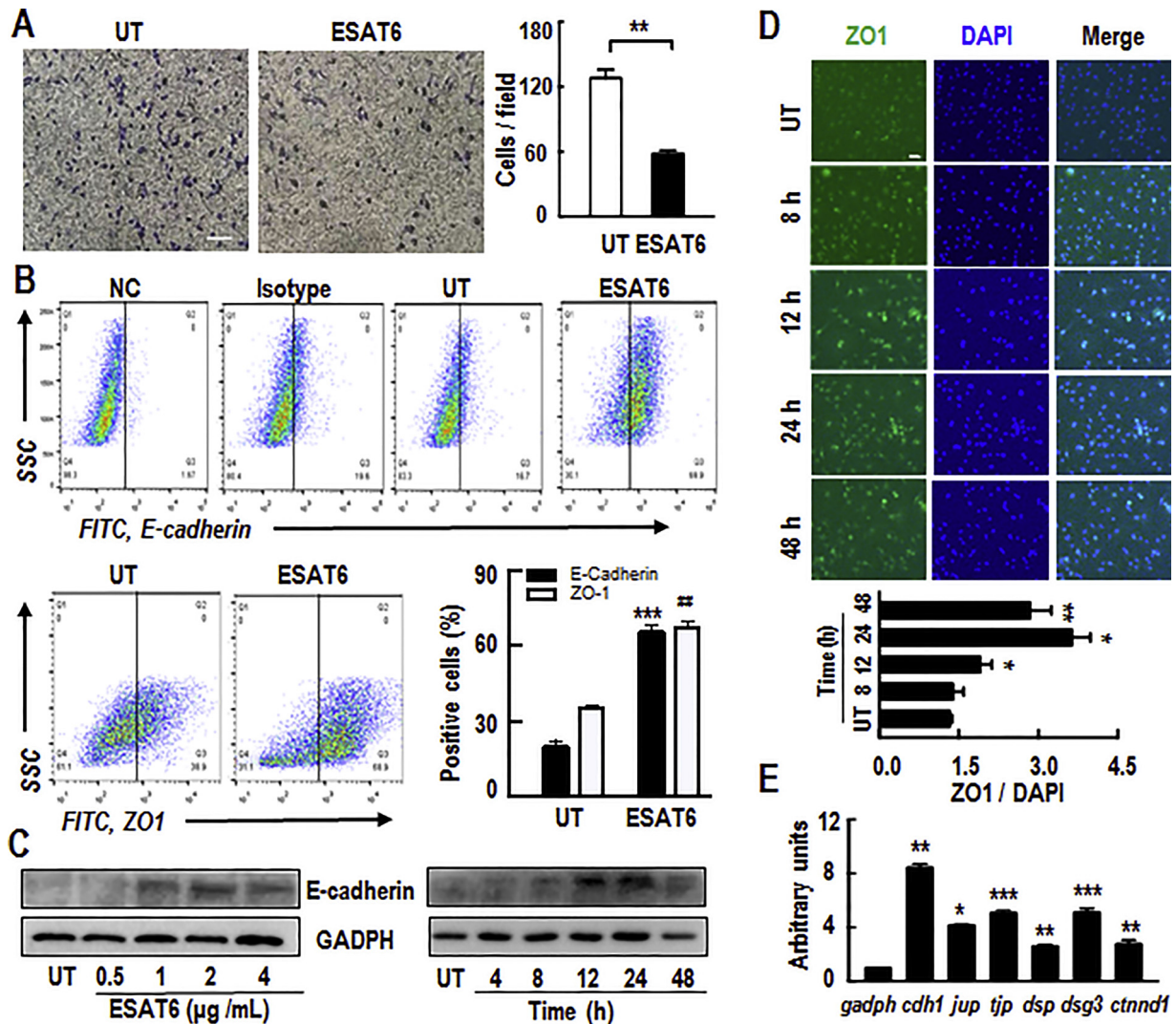


Fig. 2. ESAT6 induces the transition of BMDMs into epithelioid macrophage. **A.** The effect of ESAT6 on cell mobility. BMDMs were treated with or without 3 µg/ml ESAT6 for 24 h, then the cells migration status was observed under microscope after cells were stained with crystal violet in the transwell plate. The number of migrated cells was randomly counted in three high power fields under microscope. Bar = 50 µm. Data are represented as the mean ± SEM of three separate experiments from three individual mice. **B.** The expression of E-cadherin on the surface of BMDMs was induced by ESAT6. The cells were incubated with or without 3 µg/ml ESAT6 for 24 h. The cells were stained with FITC labeled E-cadherin antibody or ZO1 antibody before being analyzed by flow cytometry. The percentage of E-cadherin or ZO1 positive cells was calculated using Flow Jo software. Data are represented as the mean ± SEM of three separate experiments from three individual mice. **C.** ESAT6 stimulated E-cadherin protein expression from BMDMs in a dose- and time-dependent manner. BMDMs were treated with ESAT6 in a concentration range indicated for 24 h or in a time period indicated with 3 µg/ml ESAT6 treatment. Total proteins of the cells were extracted and analyzed by Western blots. GAPDH served as an internal control. A representative set of WB results was shown. Similar results were observed in three separate experiments from three individual mice. **D.** The time curve of ZO1 expression on the surface of BMDMs after the cells were stimulated with ESAT6. BMDMs were stimulated with 3 µg/ml ESAT6 for a time period indicated, then double stained with ZO1 (green) and DAPI (blue) before the cells were observed under fluorescence microscope. Bar = 50 µm. Similar results were obtained from three separate experiments from three individual mice. The immunofluorescence image was analyzed and the data of quantitative immunofluorescence ratio of ZO1/DAPI were shown in the time period. **E.** The mRNA expression levels of EMMMs genes *cdh1*, *jup*, *tjp*, *dsp*, *dsq3*, *ctndf1* in ESAT6-treated BMDMs. BMDMs were treated with or without 3 µg/ml ESAT6 for 24 h. then total RNA were extracted from the cells and the relative mRNA levels of the EMMMs genes were analyzed by qPCR. The gene expression levels were calculated by the double delta CT method (n = 6). *P < 0.05, **P < 0.01, ***P < 0.001 vs. control group.

iNOS/NO in this study, the expression level of iNOS and NO production in the ESAT6-stimulated macrophages were investigated. An increasing of iNOS expression and NO production can be seen in a time-dependent manner after BMDMs from WT mice was treated with ESAT6 in the time periods indicated (Fig.4A-B). It is worth mentioning that compared with the BMDMs from WT mice, NO was not detected in the culture supernatant of BMDMs from TLR2^{-/-} mice under the same condition of treatment (Fig.4C). These results also reveal that ESAT6-induced NO production requires TLR2 existence on the surface of macrophages. Next, BMDMs were then pretreated with SMT (an iNOS inhibitor) or PTIO (an NO inhibitor) respectively before detecting iNOS expression

or NO production in the ESAT6-treated BMDMs. The results demonstrate that the inhibition of NO production did not affect iNOS expression (Fig.4D) but iNOS inhibitor could significantly downregulate NO generation in ESAT6-treated BMDMs (Fig.4E). Furthermore, NO inhibitor PTIO could significantly downregulate the expression of E-cadherin on the surface of the cells (Fig.4F). These results clearly indicate that ESAT6-induced increment of iNOS is responsible for NO generation. Interestingly, both iNOS and NO inhibitors could also abrogate ESAT6-induced upregulation of the mRNA expression of the group of EMMMs genes in the BMDMs (Fig.4G-H). These findings indicate that ESAT6 can induce iNOS/NO production and the inhibitors of

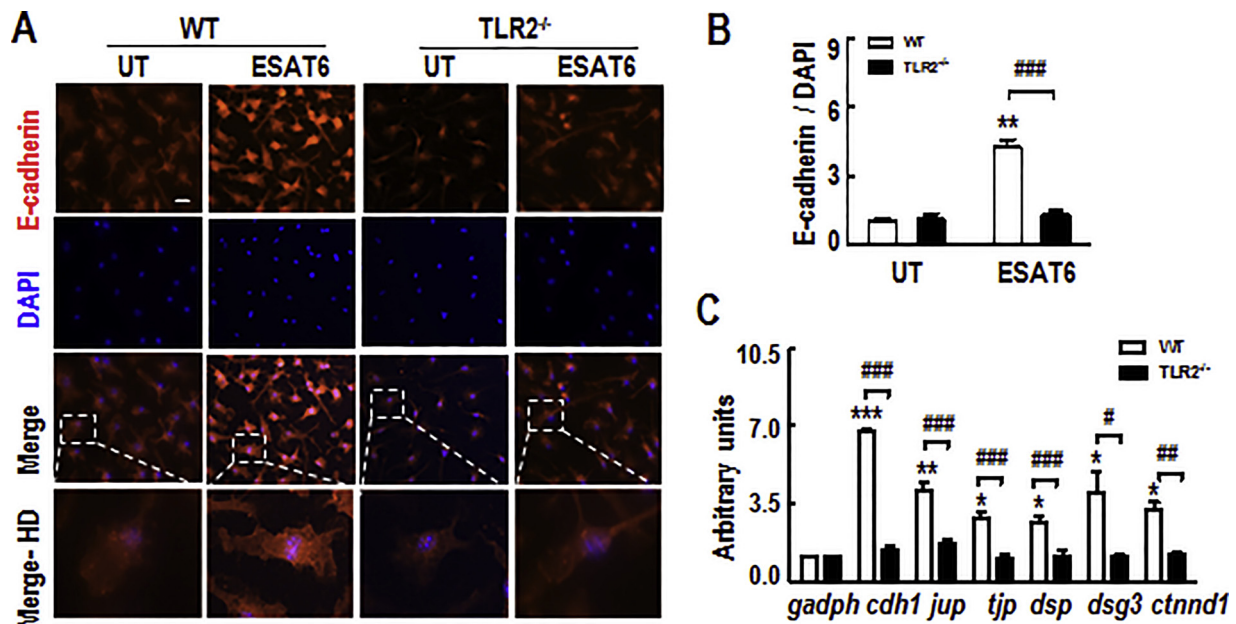


Fig. 3. TLR2 is required for ESAT6 trigger transition in macrophage.

A-B. TLR2 knock-out could impact the expression of E-cadherin in ESAT6-treated BMDMs. BMDMs from WT and TLR2^{-/-} mice were stimulated with 3 μ g/ml ESAT6 for 24 h, then the cells were stained with E-cadherin (red) and DAPI (blue). The staining results were observed by inverted fluorescence microscope. Similar results were obtained from three separate experiments from three individual mice. The immunofluorescence image was analyzed and the data of quantitative immunofluorescence ratio of E-cadherin/DAPI were shown in Fig.3B. C. Evaluation of TLR2 effect on the mRNA transcription of EMMMs genes *cdh1*, *jup*, *tjp*, *dsp*, *dsg3*, *ctndd1* in ESAT6-treated BMDMs. BMDMs from WT and TLR2^{-/-} mice were stimulated with or without 3 μ g/ml ESAT6 for 24 h. The relative genes mRNA expression levels were analyzed by qPCR. The gene expression levels were calculated by the double delta CT method (n = 6). **P* < 0.05, ***P* < 0.01, ****P* < 0.001 vs. control group. #*P* < 0.05, ##*P* < 0.01, ###*P* < 0.001 compared between WT and TLR2^{-/-} groups.

iNOS or NO could markedly inhibit the expression of EMMMs induced by ESAT6.

It has been reported that polycomb repressive complex 2 (PCR2) proteins act as evolutionary conserved epigenetic mediators of cell identity (Schuettengruber and Cavalli, 2009). A hallmark of PRC2 activity is trimethylated lysine 27 on histone H3 (H3K27me3) that inhibits mRNA transcription. EZH2, one component of PCR2, is an important regulator of macrophage activation and inflammation inducer. EZH2 could mediate the expression of multiple genes in macrophages (Zhang et al., 2018). It has been also reported that H3K27me3 has the function of downregulating epithelial cells marker protein expression (Cao et al., 2008). To identify whether H3K27me3 controls the expression of EMMMs in this study, ESAT6 induction of H3K27me3 was explored. As expected, Fig.5A shows that ESAT6 could inhibit H3K27me3 activation in BMDMs after 24 h stimulation. Interestingly, this inhibition can be blocked by the inhibitors of SMT or PTIO respectively. These results indicate that the activation of iNOS/NO is the signal for downregulating H3K27me3 in ESAT6-treated BMDMs. Furthermore, ESAT6-induced E-cadherin positive cells significantly reduced in the presence of H3K27 histone demethylase inhibitor (GSK J1) (Fig.5B). The expression mRNA levels of the group of EMMMs genes also dramatically dropped in the presence of inhibitor GSK J1 (Fig.5C). These results suggest H3K27me3 is a main factor in controlling the induction of EMMMs expression in this study.

3.4. Hypoxia inhibits transition induced by ESAT6 in macrophages

An interesting phenomenon has been observed that, in general, epithelioid cells are located around the center of a granuloma in a typical clinical granuloma sample (Beham et al., 2011). A study in Mtb infected zebrafish also shows that the formation of early epithelioid macrophages was observed around the lesion with the development of the disease. The epithelioid cells were distributed in the periphery of granuloma in a centripetal state (Cronan et al., 2016). Surprisingly,

epithelioid macrophages were not observed in the center of granuloma while the above results showed that ESAT6 could induce macrophage transition into epithelioid macrophages with uniform distribution, the mechanism of this phenomenon needs to be explored. It has been assumed that epithelioid macrophages are formed at lesion center initially in the early stage of TB infection. As known, the development of TB disease is associated with the generation of iNOS/NO, which may lead the center of the tuberculous granuloma in hypoxic condition (Galagan et al., 2013; Brüne et al., 2013). This study speculated that the hypoxia in the center of granuloma may affect the transition. To confirm this hypothesis, ROS production in the ESAT6-stimulated macrophages were investigated. The production of ROS in BMDMs increased significantly after 12 h stimulation, but there was no significant change with 6 h stimulation (Fig.6A). The study further investigated the effect of hypoxic state on ESAT6-induced macrophage transition into epithelioid macrophages. After BMDMs were pretreated with ROS scavenging agent DMTU, then the cells were further stimulated with ESAT6, and the mRNA expression levels of the group of EMMMs genes were detected by qPCR. As shown in Fig.6B, the mRNA transcription levels of the group of EMMMs genes were significantly down-regulated after the cells were pre-treated with DMTU. These results positively reveal that the expression of these EMMMs in ESAT6-treated macrophage are free oxygen ion dependent, which may partially explain why epithelioid macrophages were located around the center of the granuloma since the center is insufficient of free radical.

4. Discussion

Tuberculosis is a chronic infectious disease caused by the Mtb. The granuloma is the pathological diagnosis characteristic marker that is made up of macrophages and macrophage derivative cells. The ESAT6 encoding gene is located in the virulence coding region RD1 of Mtb, and the animal model of Mtb- Δ RD1 infection cannot form well-organized granuloma (Volkman et al., 2004), indicating that the protein encoded

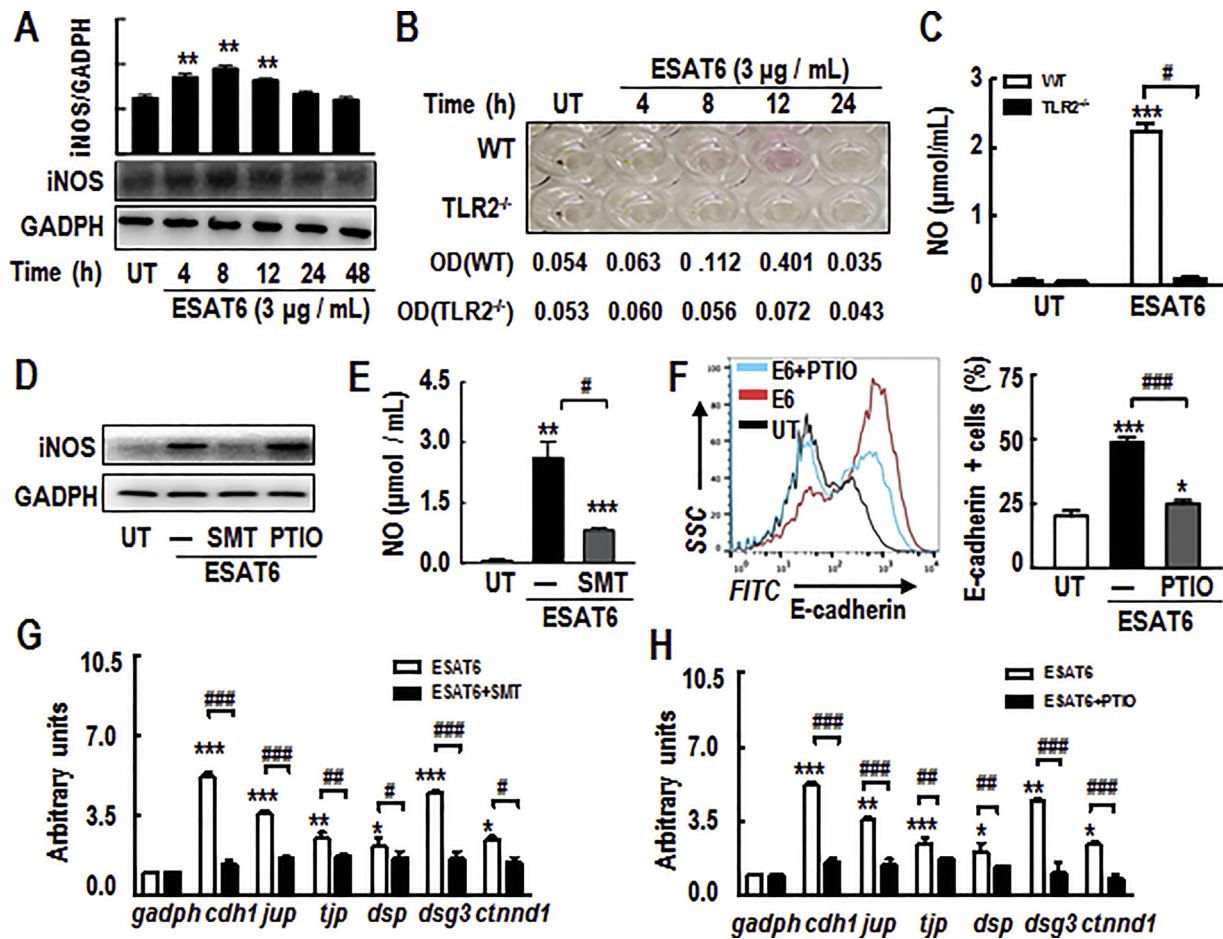


Fig. 4. ESAT6-mediated BMDMs transition is involved in iNOS/NO signaling.

A. The time curve of iNOS expression induced by ESAT6 in BMDMs. BMDMs were treated with 3 µg/ml ESAT6 for the time period indicated. Total proteins of the cells were extracted and the protein expression levels of iNOS was detected by Western blots. GAPDH served as an internal control. A representative set of WB results was shown. Similar results were observed in three separate experiments from three individual mice. B–C. The time curve of NO production induced by ESAT6 in BMDMs. BMDMs from WT and TLR2^{-/-} mice were stimulated with 3 µg/ml ESAT6 for the time period indicated. The levels of synthesized NO were measured in the supernatants and quantified by image J software. A typical stimulation time (12 h) for NO production was represented in Fig.4C (n = 4). D. The inhibitors of iNOS and NO disturb the activation of iNOS in ESAT6-stimulated BMDMs. BMDMs were pretreated with SMT (25 mM iNOS inhibitor) or PTIO (20 mM NO inhibitor) for 1 h, then the cells were further incubated with 3 µg/ml ESAT6 for 8 h. Total proteins of the cells were extracted and iNOS expression levels were analyzed by Western blots. A representative set of WB results was shown. Similar results were observed in three separate experiments from three individual mice. E. The iNOS inhibitor affects NO production in ESAT6-treated cells. BMDMs were pretreated with SMT (25 mM iNOS inhibitor) for 1 h, then the cells were further incubated with 3 µg/ml ESAT6 for 12 h. NO production levels were measured and the data are represented (n = 4). F. NO inhibitor influences the expression of E-cadherin molecule on the surface of ESAT6-stimulated BMDMs. BMDMs were pretreated with PTIO (20 mM) for 1 h before incubating with 3 µg/ml ESAT6 for 24 h. The cells were stained with FITC labeled E-cadherin antibody before being analyzed by flow cytometry. A typical E-cadherin expression on the surface of ESAT6-stimulated cells was shown and the percentage of E-cadherin positive cells was calculated using Flow Jo software (n = 4). G–H. The effect of inhibitors of iNOS or NO on the mRNA transcription of EMMMs genes *cdh1*, *jup*, *tjp*, *dsp*, *dsq3*, *ctnd1* in ESAT6-stimulated BMDMs. BMDMs were pretreated with or without SMT (25 mM iNOS inhibitor) or PTIO (20 mM NO inhibitor) for 1 h, and further incubated with 3 µg/ml ESAT6 for an additional 24 h. Total RNA were extracted and the mRNA transcription levels were analyzed by qPCR. The gene expression levels were calculated by the double delta CT method (n = 6). *P < 0.05, **P < 0.01, ***P < 0.001 vs control group. #P < 0.05, ##P < 0.01, ###P < 0.001 compared between two groups.

in RD1 region determines the formation of granuloma. Granulomas are aggregates of macrophages, including epithelioid macrophages, multi-cellular giant cells, and foam cells. The molecular mechanism of foam cells or multinucleate giant cells has been reported (Ahlwalia et al., 2017; Lay et al., 2007; Shrivastava and Bagchi, 2013). But epithelioid macrophage polarization during tuberculous granuloma formation and development has rarely been reported. In recent years, it has been reported that epithelioid macrophages are derived from macrophages (Cronan et al., 2016). However, the molecular basis and signal pathway of epithelioid macrophages formation have not been fully studied. It is also unclear whether ESAT6 encoded in RD1 regulates the formation of epithelioid macrophages. This study has demonstrated that ESAT6 can markedly upregulate the molecules expression of E-cadherin and ZO1 proteins, and increase a group of EMMMs genes expression in BMDMs,

such as *cdh1*, *jup*, *tjp*, *dsp*, *dsq3*, *ctnd1*. These effects are dependent on ESAT6 bound with TLR2 to activate the iNOS/NO signal pathway. High levels of iNOS/NO can down-regulate the methylation of H3K27me3, which increases mRNA transcription of EMMMs genes and enhances EMMMs protein expression in the macrophages. Interestingly, ROS production can also elevate expression of these molecules.

Early studies have found that interference to E-cadherin expression, a tight junction protein between epithelioid macrophages, leads to the formation of poorly organized granuloma, which results in unrestricted Mtb motion and causes Mtb proliferation and spread in the body. It has been reported that 12 molecules of epithelial cell protein markers are expressed on the epithelioid macrophages derived from the Mtb infected macrophages (Cronan et al., 2016). ESAT6 can increase integrin expression to enhance the adhesion function of macrophages and

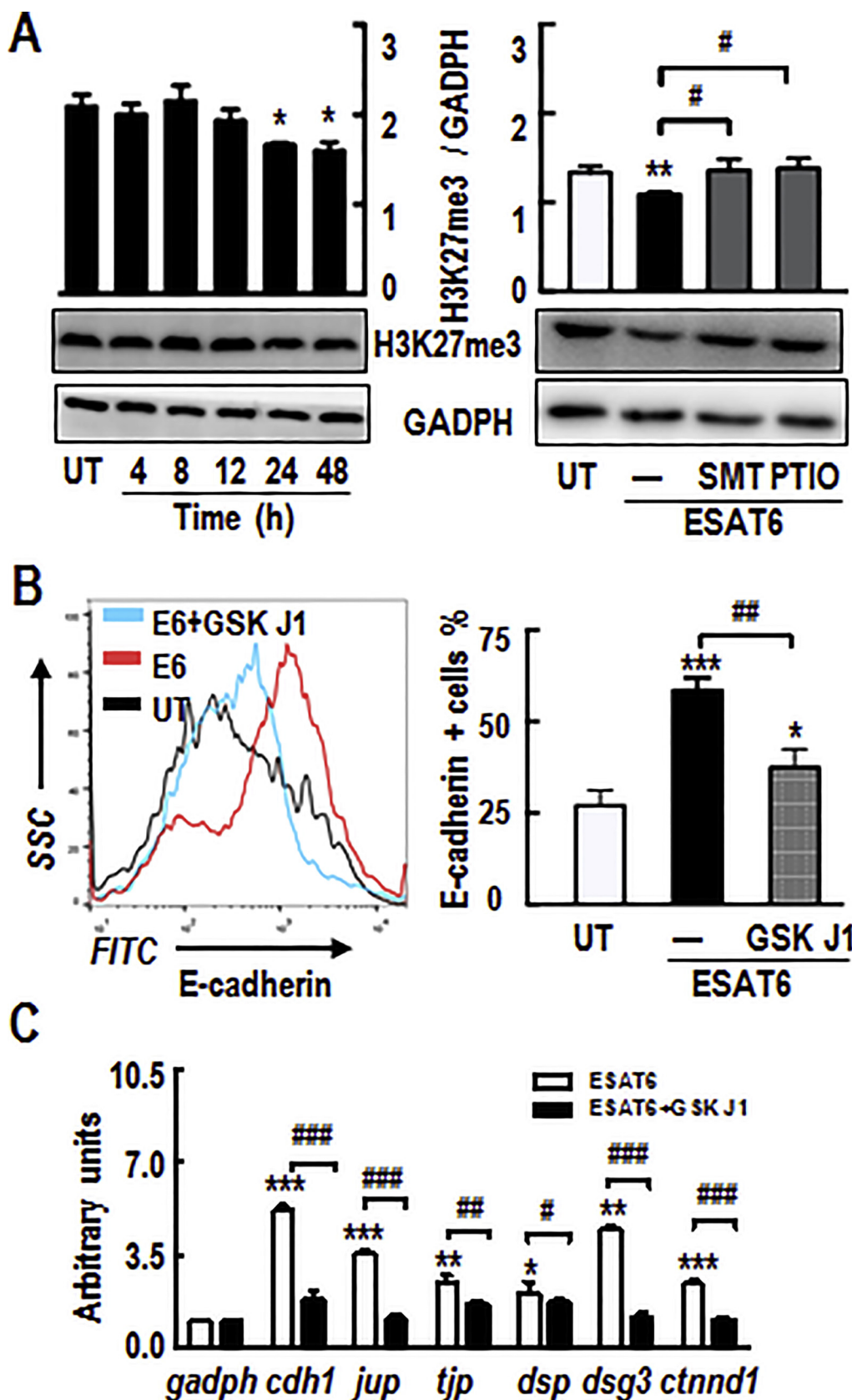


Fig. 5. The trimethylation of histone H3K27 regulates ESAT6-induced transition in macrophage.

A. The effect of iNOS or NO on the trimethylation of histone H3K27 in BMDMs stimulated by ESAT6. BMDMs were treated with 3 $\mu\text{g/ml}$ ESAT6 for the time period indicated (left), or pretreated with SMT (10 μM) or PTIO (1 mM) for 1 h, then incubating with 3 $\mu\text{g/ml}$ ESAT6 for an additional 24 h (right). Total proteins of cells were extracted and the protein levels of trimethylation status of H3K27 was detected by western blot analysis. GAPDH served as an internal control. A representative set of WB results was shown. Similar results were observed in three separate experiments from three individual mice. B. Inhibition of the methylation of H3K27 impacts the expression of E-cadherin molecule on the surface of ESAT6-stimulated BMDMs. BMDMs were preincubated with GSK J1 (40 nM) for 1 h, and then treated with 3 $\mu\text{g/ml}$ ESAT6 for an additional 24 h. The cells were then stained with FITC labeled E-cadherin antibody before being analyzed by flow cytometry. A typical E-cadherin expression on the surface of ESAT6-stimulated BMDMs was shown and the percentage of E-cadherin positive cells was calculated using Flow Jo software (n = 4). C. The inhibition of ESAT6-induced H3K27me3 in BMDMs affects the EMM genes mRNA expression. BMDMs were pretreated with GSK J1 (40 nM) for 1 h, then the cells were incubated with 3 $\mu\text{g/ml}$ ESAT6 for an additional 24 h. The relative mRNA expression levels of EMM genes *cdh1*, *jup*, *tjp*, *dsp*, *dsg3*, *ctnd1* in the cells were analyzed by qPCR. The gene expression levels were calculated by the double delta CT method (n = 6). * $p < 0.05$, ** $p < 0.01$, *** $p < 0.001$ vs. control group. # $p < 0.05$, ## $p < 0.01$, ### $p < 0.001$ compared between two groups.

further inhibit the migration ability of macrophages (Hemmati et al., 2016). This study has showed ESAT6 alone can also upregulate the expression of a group of EMM including E-cadherin, junction plagglobin, ZO1, desmoplakin, desmoglein3 and catenin proteins in

macrophage and affect the cell migration, which suggests that ESAT6 can induce macrophage to transdifferentiate into epithelioid macrophages.

It is believed that NO and ROS can adjust the immune balance inside

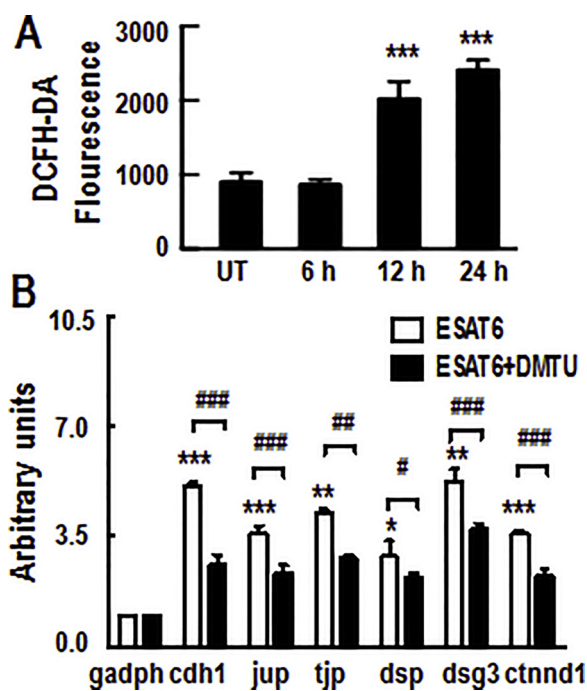


Fig. 6. The inhibitor of ROS attenuates ESAT6-induced macrophage transition. **A.** The time curve of ROS production induced by ESAT6 in BMDMs. BMDMs were treated with 3 $\mu\text{g/ml}$ ESAT6 for the time period indicated, then cells were probed with ROS indicator DCFH-DA for 30 min. The ROS production in the cells were measured by flow cytometry ($n = 6$). **B.** Effects of ROS inhibitor on ESAT6-induced EMMM genes expression. BMDMs were pretreated with ROS inhibitor DMTU (15 μM) for 1 h, then the cells were further incubated with 3 $\mu\text{g/ml}$ ESAT for an additional 24 h. The mRNA expression levels of EMMM genes *cdh1*, *jup*, *tjp*, *dsp*, *dsg3*, *ctnd1* in the cells were analyzed by qPCR. The gene expression levels were calculated by the double delta CT method ($n = 6$). * $P < 0.05$, ** $P < 0.01$, *** $P < 0.001$ vs. control group. # $P < 0.05$, ## $P < 0.01$, ### $P < 0.001$ compared between two groups.

the granuloma (Ehrt et al., 2001). ROS mediates the activation of PI3K, JNK, ERK pathway promoting the production of cytokines from macrophages to activate immune cells and control the inflammatory response. It has been confirmed that ESAT6 can directly bind to TLR2 receptor through its C terminal and induces ROS production in macrophages (Jung et al., 2017; Liu et al., 2014). This study confirms that ESAT6 has the specific plasticity of transdifferentiating macrophage into epithelioid macrophages via TLR2 although Pam3CSK4, a common TLR2 activator, can also induce low level of E-cadherin expression (data not shown). These results speculate that ESAT6 bound with TLR2 does not function as Pam3CSK4, and it may activate different signaling or other “cross-talk” to induce EMMMs expression.

An increasing body of evidence has shown that Mtb successfully evades immune clearance through limiting ROS and NO produced in macrophages, suggesting that the generation of ROS and NO plays a decisive role in the anti-Mtb infection (Ehrt et al., 2001). When macrophages are activated by LPS and IFN, they use L-arginine to synthesize NO by the activation of iNOS to play the toxic role against microorganisms (Wang et al., 2017). Interestingly, a recent study has found that NO can be used as signaling molecules regulating cell signaling pathway and biological functions (Weigert et al., 2018). A recent study has reported that the distribution of iNOS in granuloma is consistent with the localization of epithelioid cells, which suggests that iNOS is accompanied by the formation of epithelioid macrophages and the production of iNOS is crucial to the progression of TB (Landes et al., 2015). This study has found that ESAT6 could induce macrophages to express iNOS and produce NO that further regulates the expression of the group of EMMMs in epithelioid macrophages. However, a

controversial result has been reported that ESAT6 could only induce the expression of NO in IFN γ -stimulated macrophages but not in untreated macrophages (Xie et al., 2016). The reason for this difference may be due to different source of macrophages used in the experiment, which is commonly observed in many other studies (Andreu et al., 2017; Feng et al., 2008).

Methylation or acetylation of histone modification is a molecular regulation mechanism of cellular plasticity. Many studies showed that the trimethylation of H3K27 regulates epithelial cells expressing the marker proteins in Epithelial-Mesenchymal Transition (Oikawa et al., 2018). It has also been reported that NO can regulate the transition of fibroblasts into endothelial cells (Meng et al., 2016). This study confirms that the mechanism of macrophage transition into epithelioid macrophages is due to ESAT6 regulating the trimethylation state of H3K27 by NO production. From clinical aspect, epithelioid macrophages appear with the Mtb infection lesion, and the distribution was mainly located in the margin of the granuloma (Cronan et al., 2016). Mtb secretes ESAT6 mainly in the infection center and the concentration of ESAT6 should be reduced progressively from the center to the margin of the granuloma. According to the results of this study, the epithelioid macrophages should be accumulated in the infection center, which is contrary to the clinical pathological observation. Recently, more and more studies have been carried out and discovered the relationship between free oxygen ion and hypoxia in granuloma formation. It has been reported that the center of granuloma is hypoxic (Lay et al., 2007). The formation of oxygen ion is an indispensable factor in maintaining the production of NO, and hypoxia can inhibit the production of NO (Brüne et al., 2013). Interestingly, ESAT6 can induce macrophage generating ROS through TLR2 (Liu et al., 2014). This study demonstrates that the inhibition of ROS generation can successfully suppress the transition of macrophage into epithelioid macrophages induced by ESAT6. This finding may explain the pathological phenomenon that the distribution of epithelioid macrophages in the zebrafish model of Mtb infection. It has been found the distribution of epithelioid macrophages are reduced from the outside to the center of granuloma, and the epithelioid cells accumulates around the lesion (Wang et al., 2017). The production of ROS has been reported to be conducive to the aggregation of macrophages (Deffert et al., 2014), which is beneficial to the development of dense granuloma. These findings reveal an important role of ROS in the maintenance and reinforcement of granuloma structure. In other words, the transition of macrophages may also be regulated by ROS production during the formation of granuloma, which provides convincing evidence supporting this study. Meanwhile, other studies have reported that hypoxia can inhibit H3K27me3 demethylation (Chang et al., 2016). This study has also confirmed that hypoxia inhibits macrophage transition via the downregulation of a group of EMMMs expression. Taken together, these results are consistent with the presumption that hypoxia inhibits the demethylation of H3K27me3. The findings from this study reveal that ESAT6-induced transition of BMDMs into epithelioid macrophages is regulated by NO production, and the transition can be interrupted in the hypoxic environment.

5. Conclusion

The current study explored the molecular mechanism of macrophage transition into epithelioid macrophages. A model of ESAT6 via TLR2 causing the epithelial reprogramming response is summarized in Fig. 7, which describes the proposed mechanism of ESAT6 inducing macrophage transition. As can be seen from the model, ESAT6 bound with TLR2 receptor activates iNOS/NO-H3K27me3 signaling pathway to upregulate the group of EMMMs (such as, E-cadherin, junction plakoglobin, ZO1, desmoplakin, desmoglein3 and catenin) expression and induces the transition of macrophage into epithelioid macrophages. However, hypoxia can inhibit this transition. These results reveal the molecular mechanism of epithelioid macrophages formation in

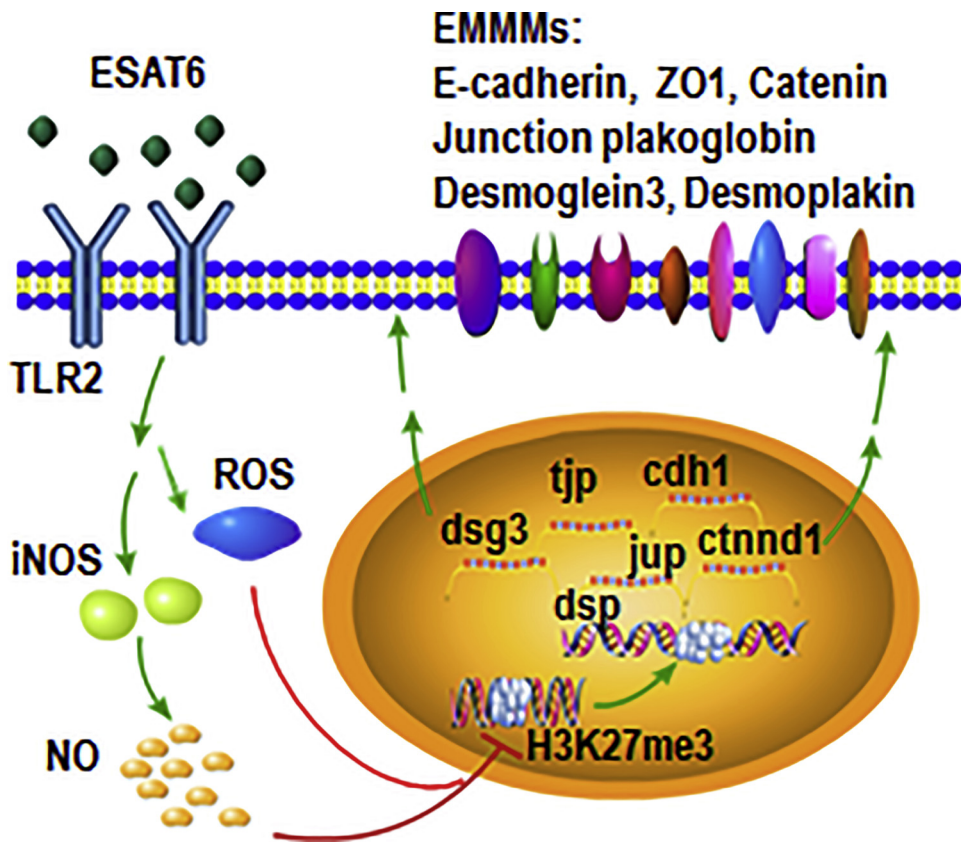


Fig. 7. A model of ESAT6 inducing expression of epithelioid macrophage marker molecules for the transition of BMDMs into epithelioid macrophages.

ESAT6, bound to TLR2 on the surface of BMDMs, can activate iNOS/NO signaling. NO further restrain H3K27me3 methylation, which increases a group of EMM genes (*cdh1*, *jup*, *tjp*, *dsp*, *dsg3* and *ctndd1*) mRNA transcription and enhances these molecules protein (E-cadherin, junction plakoglobin, ZO1, desmoplakin, desmoglein3 and catenin) expression on the surface of cells. Meanwhile, ROS production can also elevate these molecules expression. These influential actions promote the transition of BMDMs into epithelioid macrophages.

granuloma after Mtb infection, which provides new evidence of the pathogenesis of granuloma caused by Mtb and also proposes new ideas for the treatment of TB.

Declaration of Competing Interest

The authors declare that they have no conflicts of interest.

Acknowledgments

This work was supported by research fundings from Chinese National Program on Key Basic Research Project (Grant No. 2017YFA0505900) Beijing, China; and the National Natural Science Foundation of China (Grant No. 81471562) Beijing, China.

References

- Ahluwalia, P.K., Pandey, R.K., Sehajpal, P.K., Prajapati, V.K., 2017. Perturbed microRNA expression by *Mycobacterium tuberculosis* promotes macrophage polarization leading to pro-survival foam cell. *Front. Immunol.* 8, 107. <https://doi.org/10.3389/fimmu.2017.00107>.
- Andreu, N., Phelan, J., De Sessions, P.F., Cliff, J.M., Clark, T.G., Hibberd, M.L., 2017. Primary macrophages and J774 cells respond differently to infection with *Mycobacterium tuberculosis*. *Sci. Rep.* 7, 4225. <https://doi.org/10.1038/srep42225>.
- Beham, A.W., Puellmann, K., Laird, R., Fuchs, T., Streich, R., Breyssach, C., Raddatz, D., Oniga, S., Peccerella, T., Findeisen, P., Kzhyshkowska, J., Gratchev, A., Schweyer, S., Saunders, B., Wessels, J.T., Möbius, W., Keane, J., Becker, H., Ganser, A., Neumaier, M., Kaminski, W.E., 2011. A TNF-regulated recombinatorial macrophage immune receptor implicated in granuloma formation in tuberculosis. *PLoS Pathog.* 7, e1002375. <https://doi.org/10.1371/journal.ppat.1002375>.
- Brodin, P., Rosenkrands, I., Andersen, P., Cole, S.T., Brosch, R., 2004. ESAT-6 proteins: Protective antigens and virulence factors? *Trends Microbiol.* 12, 500–508. <https://doi.org/10.1016/j.tim.2004.09.007>.
- Brosch, R., Gordon, S.V., Marmiesse, M., Brodin, P., Buchrieser, C., Eiglmeier, K., Garnier, T., Gutierrez, C., Hewinson, G., Kremer, K., Parsons, L.M., Pym, A.S., Samper, S., van Soolingen, D., Cole, S.T., 2002. A new evolutionary scenario for the *Mycobacterium tuberculosis* complex. *Proc. Natl. Acad. Sci.* 99, 3684–3689. <https://doi.org/10.1073/pnas.052548299>.
- Brüne, B., Dehne, N., Grossmann, N., Jung, M., Namgaladze, D., Schmid, T., von Andreas,

- K., Weigert, A., 2013. Redox control of inflammation in macrophages. *Antioxid. Redox Signal.* 19, 595–637. <https://doi.org/10.1089/ars.2012.4785>.
- Cambier, C.J., Falkow, S., Ramakrishnan, L., 2014. Host evasion and exploitation schemes of *Mycobacterium tuberculosis*. *Cell* 159, 1497–1509. <https://doi.org/10.1016/j.cell.2014.11.024>.
- Cao, Q., Yu, J., Dhanasekaran, S.M., Kim, J.H., Mani, R.S., Tomlins, S.A., Mehra, R., Laxman, B., Cao, X., Yu, J., Kleer, C.G., Varambally, S., Chinnaiyan, A.M., 2008. Repression of E-cadherin by the polycomb group protein EZH2 in cancer. *Oncogene* 27, 7274–7284. <https://doi.org/10.1038/onc.2008.333>.
- Chang, S., Park, B., Choi, K., Moon, Y., Lee, H.Y., Park, H., 2016. Hypoxic reprogramming of H3K27me3 and H3K4me3 at the INK4A locus. *FEBS Lett.* 590, 3407–3415. <https://doi.org/10.1002/1873-3468.12375>.
- Cronan, M.R., Beerman, R.W., Rosenberg, A.F., Saelens, J.W., Johnson, M.G., Oehlers, S.H., Oehlers, S.H., Sisk, D.M., Jurcic, S.K.L., Medvitz, N.A., Miller, S.E., Trinh, L.A., Fraser, S.E., Madden, J.F., Turner, J., Stout, J.E., Lee, S., Tobin, D.M., 2016. Macrophage epithelial reprogramming underlies mycobacterial granuloma formation and promotes infection. *Immunity* 45, 861–876. <https://doi.org/10.1016/j.immuni.2016.09.014>.
- Defert, C., Schäppi, M.G., Pache, J.C., Cachat, J., Vesin, D., Bisig, R., Ma, M.X., Kelkka, T., Holmdahl, R., Garcia, I., Olleros, M.L., Krause, K.H., 2014. *Bacillus calmette-guérin* infection in NADPH oxidase deficiency: defective mycobacterial sequestration and granuloma formation. *PLoS Pathog.* 10, e1004325. <https://doi.org/10.1371/journal.ppat.1004325>.
- Ehrt, S., Schnappinger, D., Bekiranov, S., Drenkow, J., Shi, S., Gingeras, T.R., Gaasterland, T., Schoolnik, G., Nathan, C., Nathan, C., 2001. Reprogramming of the macrophage transcriptome in response to interferon-gamma and *Mycobacterium tuberculosis*: signaling roles of nitric oxide synthase-2 and phagocyte oxidase. *J. Exp. Med.* 194, 1123–1140. <https://doi.org/10.1084/jem.194.8.1123>.
- Eum, S.Y., Kong, J.H., Hong, M.S., Lee, Y.J., Kim, J.H., Hwang, S.H., Cho, S.N., Via, L.E., Barry, C.E., 2010. Neutrophils are the predominant infected phagocytic cells in the airways of patients with active pulmonary TB. *Chest* 137, 122. <https://doi.org/10.1378/chest.09-0903>.
- Feng, Y., Yang, X., Liu, Z., Liu, Y., Su, B., Ding, Y., Qin, L., Yang, H., Zheng, R., Hu, Z., 2008. Continuous treatment with recombinant *Mycobacterium tuberculosis* CFP-10-ESAT-6 protein activated human monocyte while deactivated LPS-stimulated macrophage. *Biochem. Biophys. Res. Commun.* 365, 534–540. <https://doi.org/10.1016/j.bbrc.2007.11.022>.
- Galagan, J.E., Minch, K., Peterson, M., Lyubetskaya, A., Azizi, E., Sweet, L., Gomes, A., Rustad, T., Dolganov, G., Glotova, I., Abeel, T., Mahwinney, C., Kennedy, A.D., Allard, R., Brabant, W., Krueger, A., Jaini, S., Honda, B., Yu, W.H., Hickey, M.J., Zuckler, J., Garay, C., Weiner, B., Sisk, P., Stolte, C., Winkler, J.K., Van, D.P.Y., Iazzetti, P., Camacho, D., Dreyfuss, J., Liu, Y., Dorhoi, A., Mollenkopf, H.J., Drogaris, P., Lamontagne, J., Zhou, Y., Piquenot, J., Park, S.T., Raman, S., Kaufmann, S.H.E., Mohnhey, R.P., Chelsky, D., Branch, M.D., Sherman, D.R., Schoolnik, G.K., 2013. The

- Mycobacterium tuberculosis regulatory network and hypoxia. *Nature* 499, 178–183. <https://doi.org/10.1038/nature12337>.
- Gharun, K., Senges, J., Seidl, M., Lösslein, A., Kolter, J., Lohrmann, F., Fliegau, M., Elgizouli, M., Alber, M., Vavra, M., Schachtrup, K., Illert, A.L., Gilleron, M., Kirschning, C.J., Triantafyllou, A., Henneke, P., 2018. Mycobacteria exploit nitric oxide-induced transformation of macrophages into permissive giant cells. *EMBO Rep.* 18, e201744121. <https://doi.org/10.15252/embr.201847190>.
- Gheldof, A., Berx, G., 2013. Cadherins and epithelial-to-mesenchymal transition. *Prog. Mol. Biol. Transl. Sci.* 116, 317. <https://doi.org/10.1016/B978-0-12-394311-8.00014-5>.
- Hemmati, M., Seghatoleslam, A., Rasti, M., Ebadat, S., Naghibalhosseini, F., Mostafavi-Pour, Z., 2016. Additive effect of recombinant Mycobacterium tuberculosis ESAT-6 protein and ESAT-6/CFP-10 fusion protein in adhesion of macrophages through fibronectin receptors. *J. Microbiol. Immunol. Infect.* 49, 249–256. <https://doi.org/10.1016/j.jmii.2014.06.002>.
- Jung, B.G., Wang, X., Yi, N., Ma, J., Turner, J., Samten, B., 2017. Early secreted antigenic target of 6-kDa of Mycobacterium tuberculosis stimulates IL-6 production by macrophages through activation of STAT3. *Sci. Rep.* 7, 40984. <https://doi.org/10.1038/srep40984>.
- Ke, X.S., Qu, Y., Cheng, Y., Li, W.C., Rotter, V., Øyan, A.M., Kalland, K.H., 2010. Global profiling of histone and DNA methylation reveals epigenetic-based regulation of gene expression during epithelial to mesenchymal transition in prostate cells. *BMC Genomics* 11, 669. <https://doi.org/10.1186/1471-2164-11-669>.
- Landes, M.B., Rajaram, M.V.S., Nguyen, H., Schlesinger, L.S., 2015. Role for NOD2 in Mycobacterium tuberculosis-induced iNOS expression and NO production in human macrophages. *J. Leukoc. Biol.* 97, 1111–1119. <https://doi.org/10.1189/jlb.3a1114-557r>.
- Lay, G., Poquet, Y., Salek-Peyron, P., Puissegur, M.P., Botanch, C., Bon, H., Levillain, F., Duteyrat, J.L., Emile, J.F., Altare, F., 2007. Langhans giant cells from M. Tuberculosis-induced human granulomas cannot mediate mycobacterial uptake. *J. Pathol.* 211, 76–85. <https://doi.org/10.1002/path.2092>.
- Liu, W., Peng, Y., Yin, Y., Zhou, Z., Zhou, W., Dai, Y., 2014. The involvement of NADPH oxidase-mediated ROS in cytokine secretion from macrophages induced by Mycobacterium tuberculosis ESAT-6. *Inflammation* 37, 880–892. <https://doi.org/10.1007/s10753-013-9808-7>.
- Marakalala, M.J., Raju, R.M., Sharma, K., Zhang, Y.J., Eugenin, E.A., Prideaux, B., Daudelin, I.B., Chen, P.Y., Booty, M.G., Kim, J.H., Eum, S.Y., Via, L.E., Behar, S.M., Barry, C.E., Mann, M., Dartois, V., Rubin, E.J., 2016. Inflammatory signaling in human tuberculosis granulomas is spatially organized. *Nat. Med.* 22, 531–538. <https://doi.org/10.1038/nm.4073>.
- Meng, S., Zhou, G., Gu, Q., Chanda, P.K., Ospino, F., Cooke, J.P., 2016. Transdifferentiation requires iNOS activation: role of RING1A S-Nitrosylation. *Circ. Res.* 119, e129. <https://doi.org/10.1161/CIRCRESAHA.116.308263>.
- Ohno, H., Zhu, G., Mohan, V.P., Chu, D., Kohno, S., Jacobs, W.R., Chan, J., 2003. The effects of reactive nitrogen intermediates on gene expression in Mycobacterium tuberculosis. *Cell. Microbiol.* 5, 637–648. <https://doi.org/10.1046/j.1462-5822.2003.00307.x>.
- Oikawa, T., Otsuka, Y., Onodera, Y., Horikawa, M., Handa, H., Hashimoto, S., Suzuki, Y., Sabe, H., 2018. Necessity of p53-binding to the CDH1 locus for its expression defines two epithelial cell types differing in their integrity. *Sci. Rep.* 8, 1595. <https://doi.org/10.1038/s41598-018-20043-7>.
- Pathak, S.K., Basu, S., Basu, K.K., Banerjee, A., Pathak, S., Bhattacharyya, A., Kaisho, T., Kundu, M., Basu, J., 2007. Direct extracellular interaction between the early secreted antigen ESAT-6 of Mycobacterium tuberculosis and TLR2 inhibits TLR signaling in macrophages. *Nat. Immunol.* 8, 610–618. <https://doi.org/10.1038/ni1468>.
- Pym, A.S., Brodin, P., Brosch, R., Huerre, M., Cole, S.T., 2002. Loss of RD1 contributed to the attenuation of the live tuberculosis vaccines Mycobacterium bovis BCG and Mycobacterium microti. *Mol. Microbiol.* 46, 709–717. <https://doi.org/10.1046/j.1365-2958.2002.03237.x>.
- Ramakrishnan, L., 2012. Revisiting the role of the granuloma in tuberculosis. *Nat. Rev. Immunol.* 12, 352–366. <https://doi.org/10.1038/nri3211>.
- Russell, D.G., Cardona, P.J., Kim, M.J., Allain, S., Altare, F., 2009. Foamy macrophages and the progression of the human tuberculosis granuloma. *Nat. Immunol.* 10, 943–948. <https://doi.org/10.1038/ni.1781>.
- Schuettengruber, B., Cavalli, G., 2009. Recruitment of Polycomb group complexes and their role in the dynamic regulation of cell fate choice. *Development* 136, 3531–3542. <https://doi.org/10.1242/dev.033902>.
- Sherman, D.R., Guinn, K.M., Hickey, M.J., Mathur, S.K., Zakel, K.L., Smith, S., 2004. Mycobacterium tuberculosis H37Rv:ΔRD1 is more virulent than M. Bovis bacille calmette-guérin in long-term murine infection. *J. Infect. Dis.* 190, 123–126. <https://doi.org/10.1086/421472>.
- Shrivastava, P., Bagchi, T., 2013. IL-10 modulates in vitro multinucleate giant cell formation in human tuberculosis. *PLoS One* 8, e77680. <https://doi.org/10.1371/journal.pone.0077680>.
- Silva Miranda, M., Breiman, A., Allain, S., Deknuydt, F., Altare, F., 2012. The Tuberculous Granuloma: An Unsuccessful Host Defence Mechanism Providing a Safety Shelter for the Bacteria? *Clin. Dev. Immunol.* 2012, 139127. <https://doi.org/10.1155/2012/139127>.
- Teo, J.W.P., Cheng, J.W.S., Jureen, R., Lin, R.T.P., 2013. Clinical utility of RD1, RD9 and hsp65 based PCR assay for the identification of BCG in vaccinated children. *BMC Res. Notes* 6–434. <http://www.biomedcentral.com/1756-0500/6/434>.
- Van Zyl, L., Du Plessis, J., Viljoen, J., 2015. Cutaneous tuberculosis overview and current treatment regimens. *Tuberculosis* 95, 629–638. <https://doi.org/10.1016/j.tube.2014.12.006>.
- Volkman, H.E., Clay, H., Beery, D., Chang, J.C.W., Sherman, D.R., Ramakrishnan, L., 2004. Tuberculous granuloma formation is enhanced by a Mycobacterium virulence determinant. *PLoS Biol.* 2, e367. <https://doi.org/10.1371/journal.pbio.0020367>.
- Volkman, H.E., Pozos, T.C., Zheng, J., Davis, J.M., Rawls, J.F., Ramakrishnan, L., 2010. Tuberculous granuloma induction via interaction of a bacterial secreted protein with host epithelium. *Science* 327, 466–469. <https://doi.org/10.1126/science.1179663>.
- Wang, S., Cao, M., Xu, S., Zhang, J., Wang, Z., Mao, X., Mao, X., Yao, X., Liu, C., 2017. Effect of luteolin on inflammatory responses in RAW264.7 macrophages activated with LPS and IFN-γ. *J. Funct. Foods* 32, 123–130. <https://doi.org/10.1016/j.jff.2017.02.018>.
- Weigert, A., von Knechten, A., Fuhrmann, D., Dehne, N., Brüne, B., 2018. Redox-signals and macrophage biology. *Mol. Aspects Med.* 63, 70–87. <https://doi.org/10.1016/j.mam.2018.01.003>.
- Xie, X., Han, M., Zhang, L., Liu, L., Gu, Z., Yang, M., Yang, H., 2016. Effects of mycobacterium tuberculosis ESAT6-CFP10 protein on cell viability and production of nitric oxide in alveolar macrophages. *Jundishapur J. Microbiol.* 9, e33264. <https://doi.org/10.5812/jjm.33264>.
- Yang, X., Pursell, B., Lu, S., Chang, T.K., Mercurio, A.M., 2009. Regulation of beta 4-integrin expression by epigenetic modifications in the mammary gland and during the epithelial-to-mesenchymal transition. *J. Cell. Sci.* 122 (Pt 14), 2473–2480. <https://doi.org/10.1242/jcs.049148>.
- Zhang, X., Wang, Y., Yuan, J., Li, N., Pei, S., Xu, J., Luo, X., Mao, C., Liu, J., Yu, T., Gan, S., Zheng, Q., Liang, Y., Guo, W., Qiu, J., Constantin, G., Jin, J., Qin, J., Xiao, Y., 2018. Macrophage/microglial Ezh2 facilitates autoimmune inflammation through inhibition of Socs3. *J. Exp. Med.* 215, 1365–1382. <https://doi.org/10.1084/jem.20171417>.